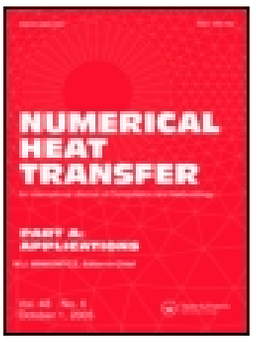

Taylor & Francis
Taylor & Francis Group

Numerical Heat Transfer, Part A: Applications
An International Journal of Computation and Methodology

ISSN: 1040-7782 (Print) 1521-0634 (Online) Journal homepage: http://www.tandfonline.com/loi/unht20

Numerical study of natural convection in asymmetrically heated channel considering thermal stratification and surface radiation

Delphine Ramalingom, Pierre-Henri Cocquet & Alain Bastide

To cite this article: Delphine Ramalingom, Pierre-Henri Cocquet & Alain Bastide (2017): Numerical study of natural convection in asymmetrically heated channel considering thermal stratification and surface radiation, Numerical Heat Transfer, Part A: Applications, DOI: 10.1080/10407782.2017.1400337

To link to this article: https://doi.org/10.1080/10407782.2017.1400337

Published online: 27 Nov 2017.

NUMERICAL HEAT TRANSFER, PART A
https://doi.org/10.1080/10407782.2017.1400337

Taylor & Francis
Taylor & Francis Group

Numerical study of natural convection in asymmetrically heated channel considering thermal stratification and surface radiation

Delphine Ramalingom, Pierre-Henri Cocquet, and Alain Bastide

Université de La Réunion, Laboratoire PIMENT, Le Tampon, France

ABSTRACT

This article consists in a numerical study of the influence of thermal stratification and surface radiation on laminar airflow induced by natural convection in vertical, asymmetrically heated channels. Several cases are investigated to spotlight their influence on fluid dynamics and thermal quantities. Thermal stratification is obtained by a weak gradient of temperature outside of the channel, and then the temperature at the bottom end of the channel is considered as a function of time. Significant effects on vertical velocities, mass flow, and flow structure are shown. Surface radiation is also considered but appears less predominant than thermal stratification for the selected conditions of this article. The impact on heat transfer is also evaluated for each studied configuration. It is observed that local and mean Nusselt numbers weakly increase for the investigated cases.

ARTICLE HISTORY
Received 31 July 2017
Accepted 26 October 2017

1. Introduction

Fluid flow and heat transfer between two vertical plates have applications in many widely used engineering systems; for example, cooling and heating industrial and electronic equipment such as transistors, mainframe computers, plate heat exchangers, solar energy collectors, and cooling of nuclear reactor fuel elements. The problem of natural convection in vertical channels has been the focus of extensive investigations because the precursory experimental works performed by Elenbaas [1]. Authors studied free convection between vertical flat plates with symmetric or asymmetric heating, with uniform heat fluxes or constant temperatures. Numerically, they proposed two main approaches to solve the problem of natural convection flow in the channel : either a complete simulation of the channel and its external environment, or a truncated simulation considering the single channel with its geometric limitations. Naylor et al. [2] considered a semicircular virtual extension at the entrance. Andreozzi et al. [3], Campo et al. [4] considered rectangular extensions at both ends of the channel. Their strategy consists to consider extended spatial domains at the entrance and at the exit where free stress or nonrotational flow conditions can be applied. However, natural convection flow is very sensitive to the size of the extensions. Liu and Tao [5] considered the channel in a closed reservoirs which surface is five times higher than the channel surface. Barozzi et al. [6] considered a cavity four times wider and three times longer than the channel. Gan [7] showed that the size of the computational domain influences the fluid flow. Suárez et al. [8] found that the computational domain including the whole channel must be 200 times larger and higher than the channel itself. Finally, Caltagirone [9] showed that this influence is not negligible when the fluid flow at the exit comes across the cavity wall. All these strategies lead to an increase in size of the computational domain which proves to be expensive, both in memory and in computational time. In our study,

CONTACT Delphine Ramalingom delphine.ramalingom@univ-reunion.fr Université de La Réunion, Laboratoire PIMENT, 117 Avenue du Général Ailleret, Le Tampon 97430, La Réunion, France.
Color versions of one or more of the figures in the article can be found online at www.tandfonline.com/unht.

Nomenclature

A	channel height $A = 2H$
b	channel width
d_w	depth reversal flow
g	gravitational acceleration
H	height of heated plate
$\tilde{J}$	linear system for radiosity
l_w	width of the reversal flow
$\dot{m}_{es}$	mass flow rate at the reentrance of the top-end
$\dot{m}_{out}$	mass flow rate at the exit of the top-end
Nu_1	mean Nusselt number
$Nu_{1/2}$	Nusselt number at mid-height of hot plate
p	pressure
Pr	prandtl number
q_{ri}	net radiative heat flux of surface element i
Ra_b	Rayleigh number based on b
T	temperature
U	dimensionless velocity
$\vec{v}$	velocity vector

Greek symbols

β	thermal expansion coefficient
ϵ	emissivity
κ	thermal conductivity
ν	kinematic viscosity
Φ	heat flux at the hot plate
σ	Stefan–Boltzmann constant
θ	dimensionless temperature

Subscripts

$_{inlet}$	bottom-end of the channel
$_{outlet}$	top-end of the channel
$_0$	reference
$_{CN}$	characteristic quantity

we chose to restrict the simulation to the channel height only and to model the thermal and dynamic boundary conditions at the exact aperture sections.

1.1. Boundary conditions for vertical channels

It is not obvious to set coherent boundary conditions at the geometrical limits because velocity and pressure values are not known a priori at the apertures of the channel. Desrayaud et al. [10] worked on a comparison exercise concerning the fluid flow and heat transfer in a vertical channel asymmetrically heated at a constant heat flux, without any downstream or upstream domain extensions. The effects of the four sets of open boundary conditions on fluid flow and heat transfer have been discussed. Brangeon et al. [11] implemented a numerical approach to study natural convection flows in an inclined and vertical channel. The study was based on an experimental configuration setup by Dupont et al. [12], and the comparison with their experimental data was led. They highlighted that local pressure boundary conditions provide an essentially flat velocity profile at the inlet that is in better agreement with the experimental profile, contrarily to global pressure boundary conditions. 3D effects were also studied and show negligible effects on the main upward flow but improve the prediction of the reversal flow. According to their latest results, pressure boundary conditions at the top and bottom sections based on Local Bernoulli relation were chosen in this numerical study.

1.2. Thermal stratification

Thermal stratification of the external environment is often not considered in numerical studies although experiments showed its existence. Indeed, Garnier [13] and Zoubir [14] demonstrated the establishment of a thermal stratification in the reservoir containing the channel asymmetrically heated. Hemmer et al. [15] also observed that a thermal stratification is established in the tank surrounding the channel. Despite all of these observations, it is often estimated that this parameter has a too weak influence to affect both the dynamics and heat flow. For example, Hemmer et al. [15] observed a maximum of gap temperature of the order of 0.25 K in the tank. Similarly, Polidori et al. [16] measured a 0.5°C/m thermal stratification in their tank and, as it would not present evolution during the first 5 min following the initiation of the heating device, they estimated that the thermal stratification has no influence on the dynamics of the convective flow in the channel. Daverat [17] studied the influence of thermal stratification on the fluid flow in a vertical channel. He observed a diminution of chimney effect, of the mass flow, and an increase of the temperature of the wall for a 0.4°C/m thermal stratification. According to these previous studies,

we notice that the influence of external thermal stratification on the flow in the channel can be interesting to investigate.

1.3. Flow reversal in vertical channel

The study of flow reversals in the case of pure natural convection in vertical channel was considered in only few works. Sparrow et al. [18] conducted an experiment to investigate the flow reversal in vertical parallel plates with water as the working flow. The flow reversal was formed by a pocket of recirculating flow when Ra/A ratio exceeded a certain magnitude. For the first time, the formation of pocket of recirculating flow was revealed by flow visualizations. It was found that the recirculation, fed by fluid drawn into the outlet section of the channel adjacent to the adiabatic wall, has no effect on the heat transfer at the heated wall. Chang and Lin [19] performed a numerical study to investigate the reversed flow and oscillating wake in an asymmetrically heated channel. The phenomenon of flow reversal was indicated near the upper adiabatic wall. It was more noticeable when the Rayleigh number increased. Kihm et al. [20] performed a numerical study matching smoke visualization to investigate a problem of flow reversal of natural convection in isothermal vertical walls. They identified the occurrence of the onset in the upper central region because of isothermal vertical walls, and they indicated variations of the entrance lengths with the Rayleigh numbers. Ospir et al. [21] conducted an experimental study on natural convection in an asymmetrically heated vertical plate with water as the working fluid. They investigated the evolution of flow reversal from a single cell to a final eight-shaped structure. Observations showed that the increase of the modified Rayleigh number resulted in an increase on the penetration of the flow reversal. Recently, Fu et al. [22] adopted the nonreflecting boundary, which was held at apertures considering the compressibility of fluid, to investigate the flow reversal of natural convection. The increase of the ratio of the width to the length of parallel plates makes the flow reversal became remarkable and drastic. The amount of fluid through the outlet flowing into parallel plates was gradually larger than that through the inlet flowing into parallel plates. In those situations, the fluids which were caused by the flow reversal through the outlet flowing into parallel plates, were completely through the outlet flow out of parallel plates again. These different studies on the flow reversal in the channel show that this quantity can be sensitive to several parameters.

1.4. Surface radiation

Except some studies in the literature, major of numerical investigations overlooked surface radiation in natural convection case. Similarly, we did not find in the literature any numerical studies about the combined thermal stratification in environment and surface radiation for the vertical channel case. However, Carpenter et al. [23] numerically studied the interaction of surface radiation with developing laminar natural convection in vertical parallel plate channels with asymmetric heating. They investigated the effects of five dimensionless parameters (heat flux ratio, Rayleigh number, aspect ratio, emissivity, and radiation number), and showed that radiation significantly alters the pure natural convection results because the maximum value of wall temperatures is reduced. The effect of surface radiation was reconsidered by Webb and Hill [24]. Their experiments were designed to determine local and average heat transfer characteristics for natural convection in a vertical parallel plate channel. They showed the importance of corrections for radiation and conduction losses, and they underlined the use of local thermophysical properties in correlating the data. Combined natural convection and thermal radiation in vertical parallel plate channels was experimentally investigated by Manca and Naso [25]. They showed that the effect of surface radiation is more important for asymmetric heating than for symmetric heating. Moreover, they emphasized that the flow patterns tend to those of symmetric heating for high wall emissivities. They also proposed correlations between local Nusselt numbers at various emissivities. Krishnan et al. [26] investigated experimentally laminar natural convection and surface radiation between vertical parallel plates by considering a central hot plate with high emmissivity ($\epsilon = 0.85$) and two unheated polished plates ($\epsilon = 0.05$).

This study highlights the significance of radiation at room temperature, and they proposed a correlation for the average convective wall heat transfer. Recently, Li et al. [27] first added an effect of radiation on investigating the flow reversal of natural convection in asymmetrically heated vertical channels numerically. Experimental results of Webb and Hill [24] were used as boundary conditions at the inlet and outlet of the channel. Their results showed that the general effect of surface radiation is to delete the onset of flow reversal at the top part of the channel, to diminish the temperature of the heated walls, and to increase the facing wall temperature.

1.5. Aim of the present study

This article reports a numerical study of the influence of thermal stratification and surface radiation on the laminar airflow induced by natural convection in vertical, asymmetrically heated channels. Studied case conducted by the French Research Group AMETh in Desrayaud et al. [10] on natural convection in open-ended channels is taken as the model problem for carrying out the computations. The thermal stratification is created first by setting a constant bottom temperature different from the top temperature, to obtain a weak gradient of temperature between the entrance and the exit of the channel. Then, we consider a function of the temperature at the inlet of the channel. The influence of external surface radiation is investigated by considering also temperature of gray bodies (bottom and top channel) that are set to values in agreement with thermal stratification surrounding the channel. This case-study approach makes the originality of our investigation. To our knowledge, it is also the first numerical study on vertical, asymmetrically heated channels that consider both thermal stratification and surface radiation and that evaluate their impact on natural convection. For the selected conditions of thermal stratification and radiation surface, it will be asserted that thermal stratification is a more important factor than surface radiation.

2. Problem setting

To reduce the computational time and to focus on the flow and heat transfer in the channel, we consider in this study a computational domain restricted to the channel geometry.

2.1. Model geometry

We consider a vertical parallel plate channel of width b and height $A = 2H$. One wall is partially heated at a constant and uniform heat flux Φ on its half-middle section, and the remaining walls are adiabatic (Figure 1).

The fluid flow is assumed laminar and two-dimensional. Accounting for the small relative temperature difference occurring between the heated wall and the aperture, the Navier–Stokes and energy equations are expressed with the Boussinesq approximation. The viscous dissipation term in the energy equation is neglected. The energy equation and the one dealing with radiant interchanges among surfaces are coupled through the thermal boundary conditions.

2.2. Mathematical formulation

2.2.1. Governing equations

The governing flow and heat transfer equations, written in dimensionless and conservative form, read

$$\nabla \cdot \vec{v} = 0 \tag{1}$$

$$\frac{\partial \vec{v}}{\partial t} + \nabla \cdot (\vec{v} \otimes \vec{v}) = -\nabla p + Pr\, Ra_b^{-1/2} \nabla^2 \vec{v} + Pr\, \theta \overrightarrow{e_y} \tag{2}$$

$$\frac{\partial \theta}{\partial t} + \nabla \cdot (\vec{v}\theta) = Ra_b^{-1/2}\, \nabla^2 \theta \tag{3}$$

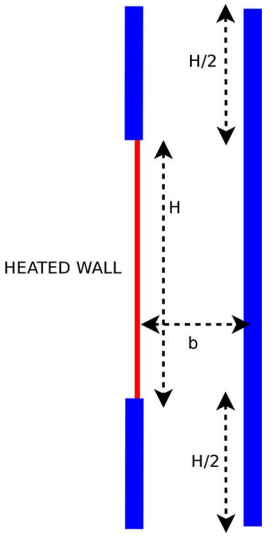

Figure 1. Geometry.

with the reduced dimensionless temperature $\theta = (T - T_0)/\Delta T$. The dimensionless parameters governing the fluid flow and heat transfer are the Prandtl number $Pr = \nu/\kappa$ and the Rayleigh number $Ra_b = g\beta\Delta T b^3/(\nu\kappa)$. The characteristic velocity is defined as $U_{CN} = \kappa Ra_b^{1/2}/b$. In this study, as the fluid treated is air, we set the Prandtl number to 0.71, except for the last configuration where the fluid is water, corresponding to a Prandtl number of 7. We also set the Rayleigh number to $Ra_b = 5{\cdot}10^5$, corresponding to a laminar flow, and the reference temperature $T_0 = 298.15$ K.

2.2.2. Surface radiation

For a given temperature distribution on the channel internal surfaces, the surface radiation problem is fully described by the linear system for radiosity $\tilde{J}_i$ $(\mathrm{W/m^2})$. The net radiative heat flux resulting from surface radiation, which is defined in the hemisphere of a surface element, can be calculated by

$$q_{r_i} = \frac{\epsilon_i}{1 - \epsilon_i}(\sigma T_i^4 - \tilde{J}_j) \ (i = 1, 2, \ldots, m) \tag{4}$$

where σ is the Stefan–Boltzmann constant, m is the total number of surface elements, and ϵ_i is the emissivity of the surface element i. In this article, we consider that the emissivity of internal walls is equal to 0.1, and the emissivity of the surfaces corresponding to the bottom end and top end is set to 0.9. The originality of this study is the temperature of bottom body and top body which are different to reference temperature. Indeed, we consider that they are located at a distance from the aperture of the channel, in a stratified ambient air.

2.3. Numerical method

The governing equations (1)–(3) are discretized with the open–source finite-volume code OpenFOAM. The pressure-implicit with splitting of operators algorithm is applied for pressure–velocity coupling. The temporal term is discretized with the second-order implicit differencing scheme. The spatial discretization is handled with a central differencing scheme, and a two-order collocated grid is adopted for the convective term in the energy equation.

2.4. Investigated configurations

Six configurations are investigated in this article (Table 1).

Table 1. Parameters of the different cases.

Case	1	2	3	4	5	6
θ_{outlet}	0	0	+0.01	0.005	0.0026	0
θ_{inlet}	0	−0.01	0	−0.005	0	$f(x,\theta)$

According to the latest results produced by Brangeon et al. [11], we chose pressure boundary conditions at the apertures based on Local Bernoulli relation:

$$p(x,y) = -\frac{1}{2}\, v(x,y)^2 \tag{5}$$

At the outlet, two cases are considered:

$$\text{if } \vec{v}\cdot\vec{n} > 0,\ p(x,y) = 0 \tag{6}$$

$$\text{else } p(x,y) = -\frac{1}{2}\, v(x,y)^2 \tag{7}$$

where $\vec{n}$ is the outward unitary normal to the fluid part of computational domain. The boundary conditions along the walls are those of Desrayaud et al. [10], that is

- imposed heat fluxes for the temperature with $\frac{\partial\theta}{\partial x} = -1$ on the heated wall, and $\frac{\partial\theta}{\partial x} = 0$ on the adiabatic walls;
- nonslip boundary conditions for the velocity.

To understand the effect of thermal stratification around the channel on natural convection, we proposed to create a weak gradient of temperature between the inlet and outlet. We consider first that the thermal stratification is a linear function. So, we set a higher dimensionless temperature at the outlet or a lower dimensionless temperature at the inlet. The last configuration corresponds to the experimental case of Hemmer et al. [15] where they measured a thermal stratification of 0.25 K in the tank containing the channel. We calculated the dimensionless temperature (0.0026), and we adapted the simulation to consider the fluid as water that means $Pr = 7$. Then, we completed the study by adding surface radiation. We assumed that temperature of bottom and top bodies are different from the reference temperature as they are in a stratified external environment. Finally, we considered the thermal stratification as a function and set it as the dimensionless temperature at the inlet of the channel. So, thermal boundary conditions at the bottom/top of the channel for the investigated configurations are the following cases:

1. **Case 1:** Reference Case
   $\theta(x, 0) = 0$ *and* $\theta(x, 2H) = 0$
2. **Case 2:** Thermal stratification case (−0.01)
   $\theta(x, 0) = -0.01$ and $\theta(x, 2H) = 0$.
3. **Case 3:** Thermal stratification case (+0.01)
   $\theta(x, 0) = 0$ and $\theta(x, 2H) = +0.01$.
4. **Case 4:** Thermal stratification case (0.005)
   $\theta(x, 0) = -0.005$ and $\theta(x, 2H) = +0.005$.
5. **Case 5:** Thermal stratification case (+0.0026) - [15] $\theta(x, 0) = 0$ and $\theta(x, 2H) = +0.0026$.
6. **Case 6:** Thermal stratification case $f(t)$
   For this last–studied-case, we define the temperature at the inlet as a function:

$$f(t) = \begin{cases} 0 & \text{if} \quad t < 100 \\ -0.01\sin^2\left(\frac{\pi}{50}(t-100)\right) & \text{if} \quad 100 < t < 150 \\ 0 & \text{if} \quad t > 150 \end{cases} \tag{8}$$

First of all, we compare dynamics and thermal quantities when we have a thermal stratified external environment. Quantities as mass flow rate exiting the channel ($\dot{m_{out}}$), mass flow rate entering through the top section ($\dot{m_{es}}$), or temperature at the inlet (θ_{outlet}) and temperature at the outlet (θ_{inlet})

are dimensionless. Second, we consider that the channel consists of four gray-diffuse, vertical surfaces (the three parts of left-hand side wall and the adiabatic right-hand side wall) and two horizontal surfaces regarded as gray radiators at an effective temperature of $T_{rad} = -0.03$ and $T_{rad} = 0.03$, respectively.

3. Results and discussions

3.1. Linear thermal stratification

3.1.1. Flow structure

Figure 2 presents the streamline patterns for the five configurations with a linear thermal stratification. As expected, we can observe a boundary layer-type flow that is developing near the heated wall due to the fluid supply from the bottom of the channel. At the same time, ambient fluid is entering the channel from the upper side of the unheated wall. This leads to the formation of a recirculation zone at the channel outlet, near the unheated wall. So, as shown in Figure 2, thermal stratification outside the channel modifies clearly the flow structure in the channel. Moreover, Table 2 provides the depth l_w and the width d_w of recirculation flow for each studied case. Compared with the Reference Case, depth of the recirculation is bigger in Case 2 and Case 4, when the temperature at the inlet is lower than T_0. The pocket-like recirculation is smaller when temperature at inlet is equal or superior to the reference temperature—for example, Case 3 and Case 5. The increase of l_w is 67.5% in Case 2 and the decrease −82.4% in Case 3. Similarly, the width d_w of the pocket-like recirculation is smaller when temperature at inlet is equal or superior to the reference temperature. For Case 2 and Case 4, considering only thermal stratification, the recirculation creates a vortex at the top section of the channel. It can be seen from Table 3 that the size of these vortex increases by considering surface radiation and setting a temperature to gray bodies. It is apparent from Tables 2 and 3 that surface radiation diminishes the effect of thermal stratification on the size of downward recirculation. The depth of recirculation pocket grows of +45.11% for Case 2 and only +9.7% in Case 4. So, thermal stratification in external environment of the channel has a significant effect on the downward flow, and its effect is mitigated through surface radiation. Yet Li et al. [27] have shown that the general effect of surface radiation is to delete the onset of pocket-like recirculation at the top part of the channel. We showed here that the effect of thermal stratification outside the channel is superior to the effect of surface radiation. So, the pocket like recirculation still exists when we take into account surface radiation in numerical simulation.

3.1.2. Vertical velocity and mass flow rate

Figures 3–7 display the vertical component of the velocity at different horizontal section of the channel. Major differences are shown at the entrance section at $y = 0$ and $y = H/4$. The centered Case 4 is the closest approximation to the Reference Case without surface radiation. We notice that vertical velocities corresponding to cases where $\theta_{inlet} < T_0$ are below to vertical velocities for cases where $\theta_{inlet} > T_0$. Case 5 with $\theta_{outlet} = +0.0026$ presents the most important velocities either the displayed section in the channel. Yet Hemmer et al. [15] considered in their study that the same thermal stratification in the tank has a too weak influence to affect the dynamics of the flow. We measured for our investigation an increase of +21.5% for the mass flow rate $\dot{m}_{out}$ in the channel (Table 2). So, our result is not in agreement with their conclusion: $\theta_{inlet} > T_0$ diminishes vertical velocity in the channel. Furthermore, we remind that for this Case 5, the fluid is water ($Pr = 7.0$) contrarily to our Reference Case ($Pr = 0.71$). At the entrance of the channel, vertical velocities consist essentially of a flat profile at entrance instead of a parabolic profile with surface radiation. This flat velocity profile at the entrance reduces the mass flow rate in the channel (Table 3). For example in Case 2, mass flow rate $\dot{m}_{out}$ decreases of −73%. As a consequence, a plug flow in the channel is produced, i.e., an effect opposite to the chimney effect. This has also been noticed by authors Daverat et al. [28] or Garnier [13]. Here, we complete their conclusion by the following result: opposite effect chimney due to thermal stratification is mitigated when we considered surface radiation.

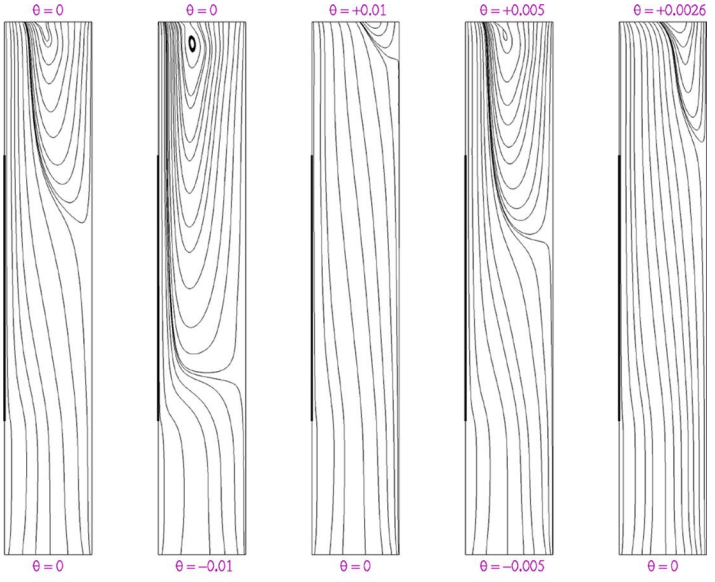

(*a*)

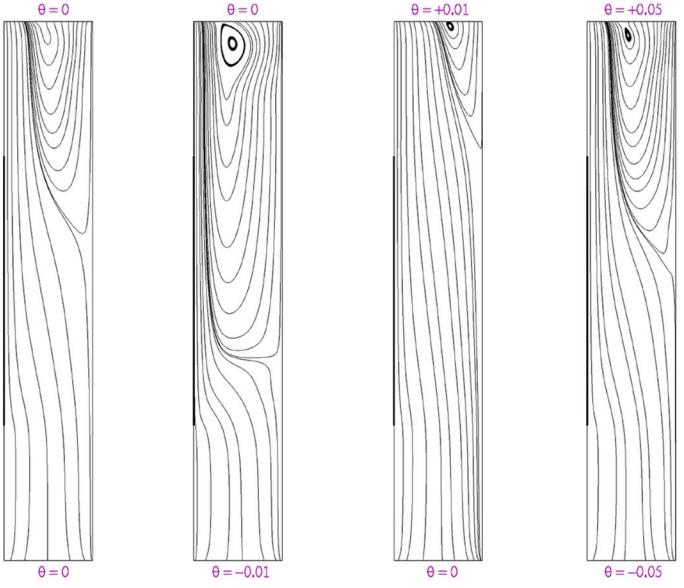

(*b*)

Figure 2. Streamtraces for (*a*) Cases 1 - 2 - 3 - 4 - 5 without radiation, (*b*) Cases 1 - 2 - 3 - 4 with radiation and TCorps.

Table 2. Dynamic quantities for case without radiation.

Case	1	2	3	4	5
$\dot{m}_{out}$	10.3	3.93	14.79	8.89	22.70
$\dot{m}_{es}$	2.79	7.76	0.26	3.22	2.02
d_w	0.61	0.70	0.32	0.63	0.55
l_w	4.05	6.78	0.71	4.10	2.95

Table 3. Dynamic quantities for Cases with radiation.

Case	1	2	3	4
$\dot{m}_{out}$	10.26	3.57	8.94	14.49
$\dot{m}_{es}$	2.86	8.63	3.20	0.27
d_w	0.60	0.70	0.39	0.63
l_w	4.30	6.24	2.43	4.72

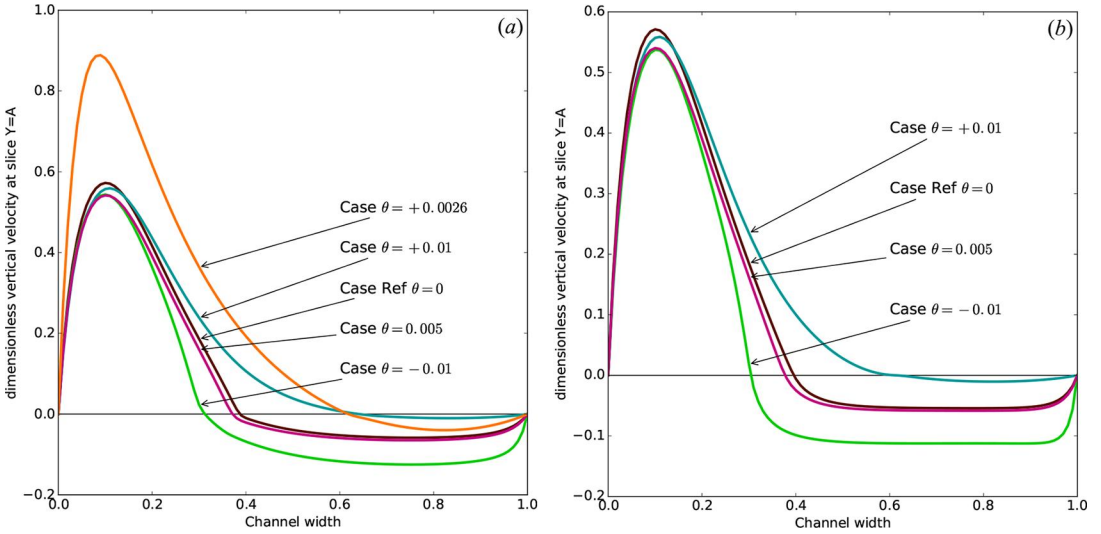

Figure 3. Vertical velocity profiles at the outlet of the channel. (*a*) Case with thermal stratification only and (*b*) Case with both thermal stratification and surface radiation.

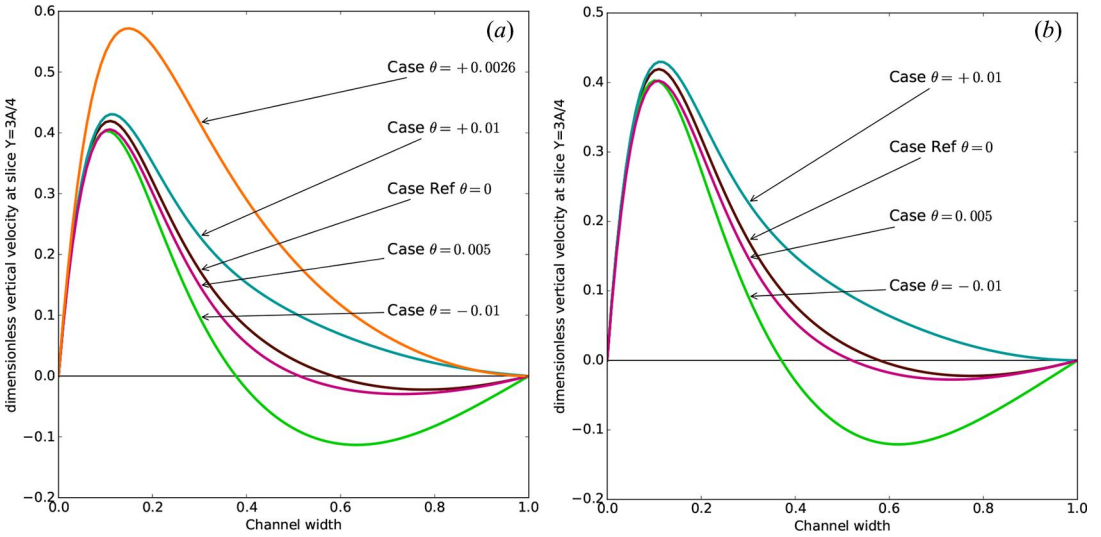

Figure 4. Vertical velocity profiles at the outlet of the heated wall. (*a*) Case with thermal stratification only and (*b*) Case with both thermal stratification and surface radiation.

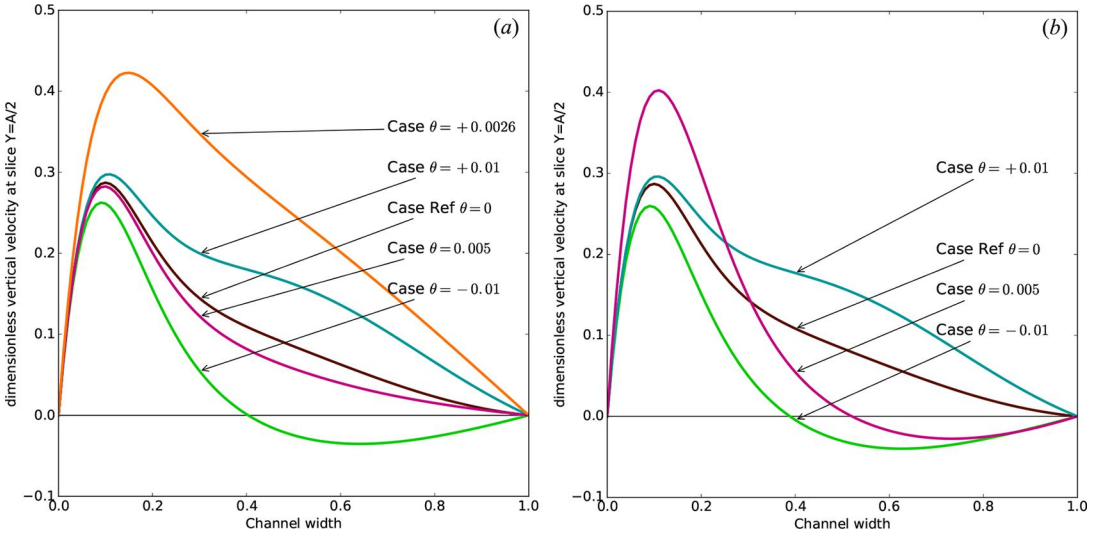

Figure 5. Vertical velocity profiles at half of the height of the channel. (*a*) Case with thermal stratification only and (*b*) Case with both thermal stratification and surface radiation.

3.1.3. Heat transfer

Temperature field is not significantly altered by thermal stratification and surface radiation. Figure 8 shows the effect of thermal stratification on the temperature distributions along the two vertical plates. As it can be seen, dimensionless temperature of right plate increases range from −0.01 below the channel bottom end to 0.01 above the channel top end. In fact, right wall temperature remains low and close to that of the fluid entering at the bottom of the channel and to the boundary conditions at the outlet. The effect of surface radiation can be seen in Figure 9. This parameter slows down the heating of the right wall. So, as observed by authors, thermal stratification and surface radiation increase slightly the temperature of right wall. However, the combined effect does not increase this

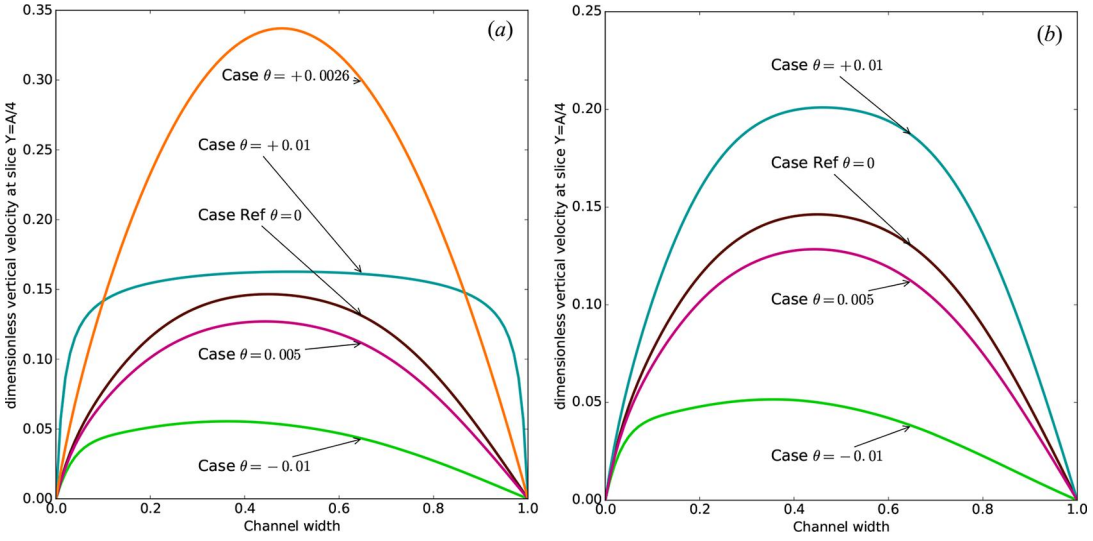

Figure 6. Vertical velocity profiles at the entrance of heated wall. (*a*) Case with thermal stratification only and (*b*) Case with both thermal stratification and surface radiation.

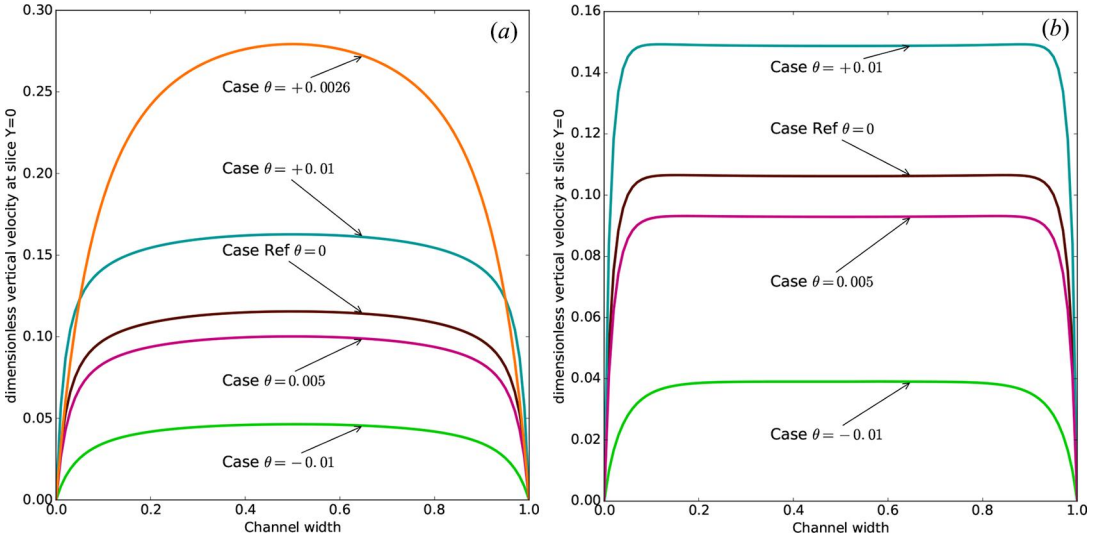

Figure 7. Vertical velocity profiles at the inlet of the channel. (*a*) Case with thermal stratification only and (*b*) Case with both thermal stratification and surface radiation.

heating. Local number ($Nu_{1/2}$) and mean Nusselt number (Nu) weakly increase for the investigated Cases (Tables 4 and 5).

3.2. Thermal stratification as a function of time

The purpose of this studied case is to investigate how the fluid flow changes with thermal stratification variation at the inlet. We considered the inlet temperature as a function of time. Figure 10 represents the dimensionless temperature at the inlet of the channel for time step from $t = 90$ to $t = 180$. So for $t \in [100, 125]$, inlet temperature decreases to the value -0.01 and for $t \in [125, 150]$, inlet temperature increases to 0. Therefore, inlet temperature is lower to the reference temperature, contrarily to the outlet temperature which is equal to T_0.

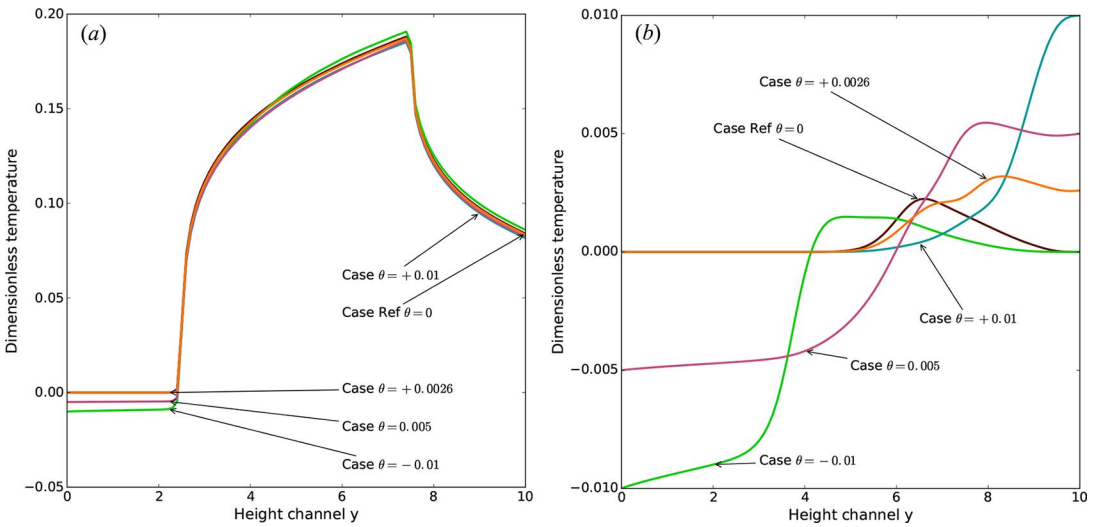

Figure 8. Dimensionless temperature of left (*a*) and right wall (*b*) - stratification Cases.

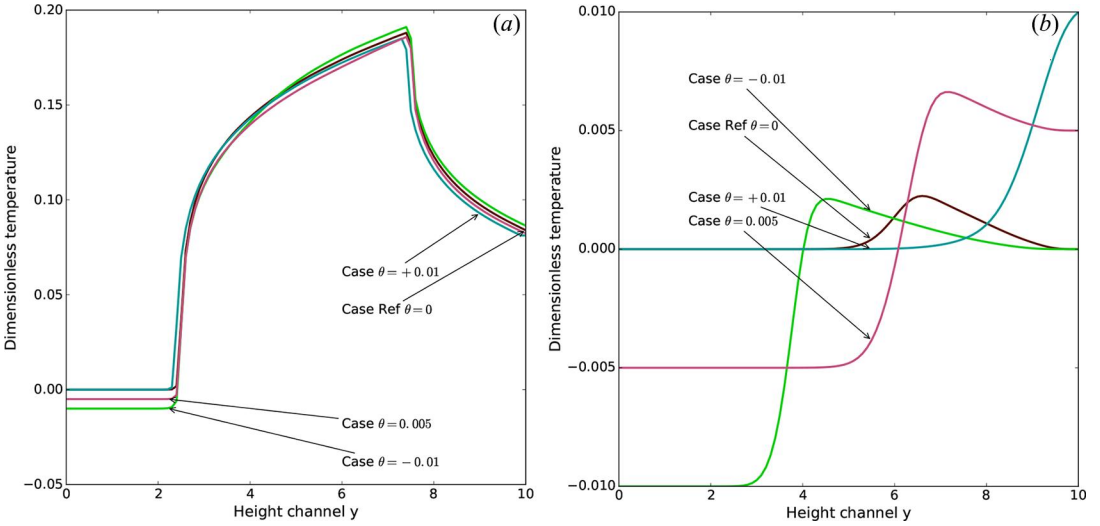

Figure 9. Dimensionless temperature of left (*a*) and right wall (*b*) - stratification and surface radiation Cases.

Table 4. Thermal quantities for Cases without radiation.

Case	1	2	3	4	5
$Nu_{1/2}$	6.20	6.16	6.31	6.34	6.24
Nu_1	6.74	6.77	6.90	6.89	6.79

Table 5. Thermal quantities for Cases with radiation.

Case	1	2	3	4
$Nu_{1/2}$	6.20	6.16	6.31	6.36
Nu_1	6.74	6.79	6.89	6.92

3.2.1. Streamlines

Changes can be observed in streamlines. Figure 11 shows different snapshots of streamlines at $t = 90$, $t = 120$, $t = 150$, and $t = 180$. A vortex is created near the adiabatic wall when temperature at the inlet

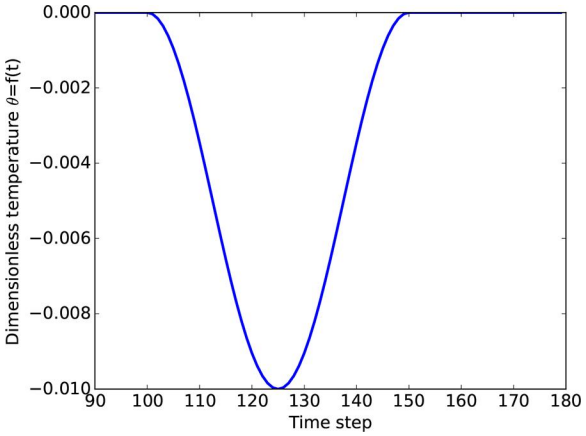

Figure 10. Thermal stratification at inlet as a function of time.

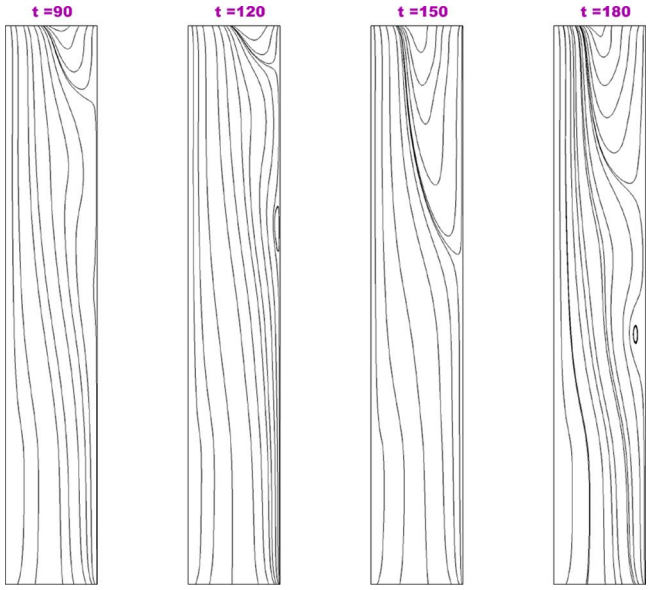

Figure 11. Streamtraces at different time step for a time function thermal stratification.

decreases. That creates an oscillation of streamlines located near the adiabatic wall. From $t = 150$, the pocket of recirculation is bigger. So, when temperature at the inlet decreases, flow enters deeper in the channel at the outlet. This increase in size of the pocket of recirculation is responsible for the creation of the vortex.

3.2.2. Mass flow rate

Figure 12 shows variation of the mass flow rate in function of time. As expected, when the temperature falls below T_0, the mass flow rate increases. As the same, when temperature increases to the value of T_0, the mass flow rate decreases. But these changes are observed with a time lag of about $t = 25$. Moreover, mass flow rate is greater than mass flow rate reached for the Case 2 which considers surface radiation. So, fluctuations of inlet temperature influence significantly the mass flow rate at the apertures.

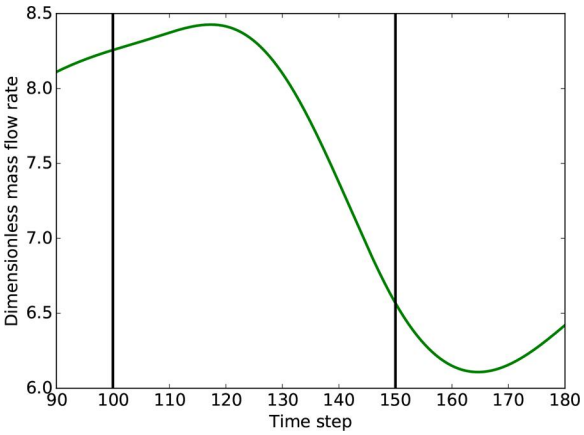

Figure 12. Variation of inlet mass flow rate in function of time.

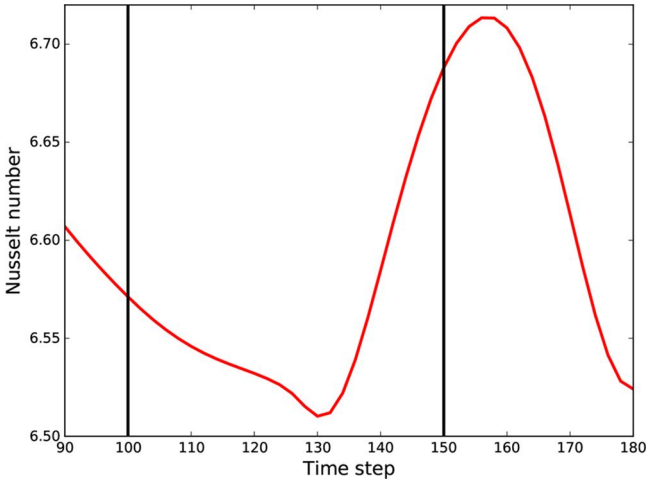

Figure 13. Variation of Nusselt number at Y = A/2 in function of time.

3.2.3. Vertical velocities

Vertical velocities are computed for probes located in the channel along the line $X = 0.5$ and represented in Figure 14. Five points are considered at different slices of the channel: $Y = 0$, $Y = A/4$, $Y = A/2$, $Y = 3A/4$, and $Y = A$. A decrease of the vertical velocity is observed for $t \in [120,130]$. That corresponds to the range in which temperature at the inlet reached its minimum, -0.01 and starts to increase. Moreover, all velocities are greater to the values reached

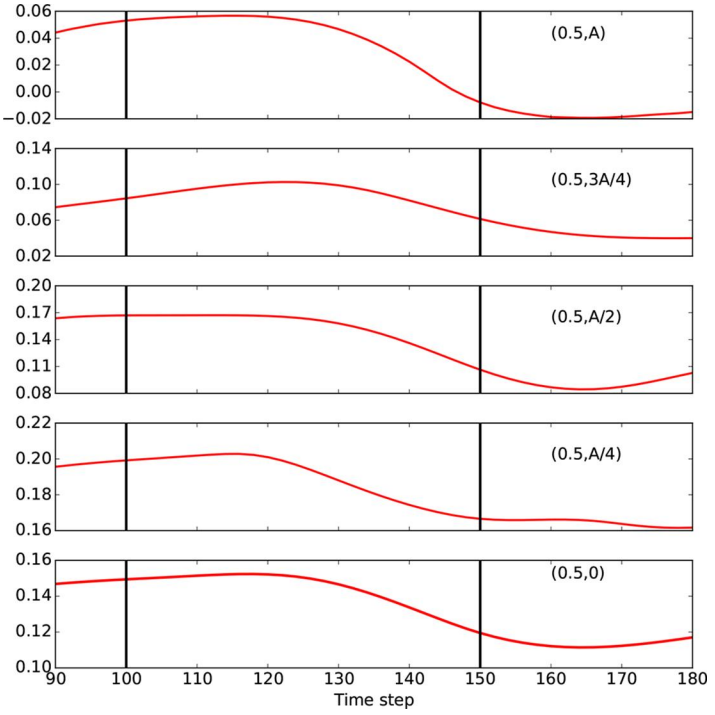

Figure 14. Evolution of vertical velocity as a function time for different probes in the channel.

in the Case 2. Indeed, respective values of velocities for each slice in Case 2 considering surface radiation are −0.11, −0.1, −0.03, 0.05, and 0.04. So, vertical velocities increased with fluctuations of inlet temperature.

3.2.4. Thermal quantities

Variation of local Nusselt number at mid-height of the hot plate in function of time (Figure 13) looks like the variation of the inlet mass flow rate in function of time. Indeed, decrease of temperature occurs an augmentation of this parameter, with a time lag of about $t = 30$. We also noticed that its value remains superior to the value reached in the Case 2 with a linear thermal stratification where $Nu_{1/2}(A/2) = 6.16$. So, fluctuations of inlet temperature increase significantly thermal quantities as the local Nusselt number at the hot plate.

4. Conclusion

Thermal stratification of the external environment and surface radiation in natural convection case are investigated numerically for vertical channel asymmetrically heated. To have a more realistic numerical simulation, we considered that gray bodies front of the apertures got a temperature different from the reference temperature T_0. Several conclusions have been drawn corresponding to the conditions of thermal stratification and surface radiation investigated.

1. Thermal stratification outside the channel and surface radiation has a significant effect on vertical velocities, mass flow rate, and flow structure.
2. Surface radiation did not suppress the existence of flow reversal in the channel because of the predominating effect of thermal stratification.
3. The effect of surface radiation reduces the effect of thermal stratification, in particular the plug effect observed by authors Daverat et al. [28] and Garnier [13].
4. The impact on dynamics and heat transfer is more important if we consider the external thermal stratification as a function of time.

In conclusion, thermal stratification and surface radiation should not be neglected in numerical simulation. We have shown that thermal quantities are mainly impacted by the variation of temperature outside the channel. Nevertheless, this numerical study considering surface radiation is limited by only one value of emissivity for the adiabatic plates. Further experimental investigations are also needed to complete and validate the findings of this research.

Acknowledgments

Computations have been performed at the University of Reunion Island supercomputer facility.

References

[1] W. Elenbaas, "Heat dissipation of parallel plates by free convection," *Physica*, vol. 9, no. 1, pp. 1–28, 1942. ISSN 00318914. DOI: 10.1016/S0031-8914(42)90053-3.
[2] D. Naylor, J. M. Floryan, and J. Do. Tarasuk, "A numerical study of developing free convection between isothermal vertical plates," *J. Heat Transfer*, vol. 113, no. 3, pp. 620–626, 1991. ISSN 0022-1481.
[3] A. Andreozzi, B. Buonomo, and O. Manca, "Numerical investigation on transient natural convection in vertical channels with heated and cooled walls," *ASME/JSME 2007 Thermal Engineering Heat Transfer Summer Conference Collocated with the ASME 2007 InterPACK Conference*, pp. 545–554. American Society of Mechanical Engineers, Vancouver, British Columbia, Canada, 2007.
[4] A. Campo, O. Manca, and B. Morrone, "Inflow and outflow effects on natural convection in partially heated vertical parallel plane channels," *ASME-IMECE*, pp. 325–335, Dallas, TX, USA, 1997.
[5] J. P. Liu and W. Q. Tao, "Numerische Ermittlung der natürlichen Konvektion um einen vertikalen Kanal in einer rechteckigen Kammer," 1996. ISSN 0947-7411.
[6] G. S. Barozzi, M. A. Corticelli, and E. Nobile, "Numerical simulation of time-dependent buoyant flows in an enclosed vertical channel," *Heat Mass Transfer*, vol. 35, no. 2, pp. 89–99, 1999. ISSN 0947-7411.

[7] G. Gan, "Simulation of buoyancy-driven natural ventilation of buildings—Impact of computational domain," *Energy Build.*, vol. 42, no. 8, pp. 1290–1300, 2010. ISSN 0378-7788.
[8] C. Suárez, P. Joubert, J. L. Molina, and F. J. Sánchez, "Heat transfer and mass flow correlations for ventilated facades," *Energy Build.*, vol. 43, no. 12, pp. 3696–3703, 2011. ISSN 03787788. DOI: 10.1016/j.enbuild.2011.10.002.
[9] J. P. P. Caltagirone, "Simulation dune expérience de thermo-convection," 2006.
[10] G. Desrayaud *et al.* "Benchmark solutions for natural convection flows in vertical channels submitted to different open boundary conditions," *Int. J. Therm. Sci.*, vol. 72(January 2009), pp. 18–33, 2013. ISSN 12900729. DOI: 10.1016/j.ijthermalsci.2013.05.003.
[11] B. Brangeon, P. Joubert, and A. Bastide, "Influence of the dynamic boundary conditions on natural convection in an asymmetrically heated channel," *Int. J. Therm. Sci.*, vol. 95, pp. 64–72, 2015. ISSN 12900729. DOI: 10.1016/j.ijthermalsci.2015.04.006.
[12] F. Dupont, F. Ternat, S. Samot, and R. Blonbou, "Two-dimension experimental study of the reverse flow in a free convection channel with active walls differentially heated," *Exp. Therm. Fluid Sci.*, vol. 47, pp. 150–157, 2013. ISSN 08941777. DOI: 10.1016/j.expthermflusci.2013.01.010.
[13] C. Garnier, "Modélisation numérique des écoulements ouverts de convection naturelle au sein d'un canal vertical asymétriquement chauffé," Ph.D. thesis, Université Pierre et Marie Curie - Paris VI, 2014. URL https://tel.archives-ouvertes.fr/tel-01127340.
[14] A. Zoubir, "Etude des transferts thermo-convectifs dans un canal semi-ouvert : Application aux façades type double-peau," Ph.D. thesis, L'institut national des sciences appliquées de Lyon, 2014. URL http://www.theses.fr/2014ISAL0003/document.
[15] C. Hemmer, C. V. Popa, A. Sergent, and G. Polidori, "Heat and fluid flow in an uneven heated chimney," *Int. J. Therm. Sci.* vol. 107, pp. 220–229, 2016. ISSN 12900729. DOI: 10.1016/j.ijthermalsci.2016.04.015.
[16] G. Polidori, S. Fatnassi, R. Ben Maad, S. Fohanno, and F. Beaumont, "Early-stage dynamics in the onset of free-convective reversal flow in an open-ended channel asymmetrically heated," *Int. J. Therm. Sci.*, vol. 88, pp. 40–46, 2014. ISSN 12900729. DOI: 10.1016/j.ijthermalsci.2014.09.011.
[17] C. Daverat, "Étude expérimentale de la convection naturelle en canal verticale à flux de chaleur imposé," Ph.D. thesis, INSA Lyon, 2012. URL http://theses.insa-lyon.fr/publication/2012ISAL0093/these.pdf.
[18] E. M. Sparrow, G. M. Chrysler, and L. F. Azevedo, "Observed flow reversals and measured-predicted Nusselt numbers for natural convection in a one-sided heated vertical channel," *J. Heat Transfer*, vol. 106, no. 2, pp. 325–332, 1984. ISSN 0022-1481.
[19] T. S. Chang and T. F. Lin, "On the reversed flow and oscillating wake in an asymmetrically heated channel," *Int. J. Numer. Methods Fluids*, 10, no. 4, pp. 443–459, 1990. ISSN 10970363. DOI: 10.1002/fld.1650100407.
[20] K. D. Kihm, J. H. Kim, and L. S. Fletcher, "Onset of flow reversal and penetration length of natural convective flow between isothermal vertical walls," *Trans. Am. Soc. Mech. Eng. J. Heat Transfer*, vol. 117, p. 776, 1995. ISSN 0022-1481.
[21] D. Ospir, C. Popa, C. Chereches, G. Polidori, and S. Fohanno, "Flow visualization of natural convection in a vertical channel with asymmetric heating," *Int. Commun. Heat Mass Transfer*, vol. 39, pp. 486–493, 2012.
[22] W. S. Fu, S. H. Huang, and C. G. Li, "An investigation of unsteady flow reversal of natural convection in vertical parallel plates by the modified local one-dimensional inviscid relations method," *Int. J. Heat Mass Transfer*, vol. 86, pp. 124–138, 2015. ISSN 00179310. DOI: 10.1016/j.ijheatmasstransfer.2015.02.032.
[23] J. R. Carpenter, D. G. Briggs, and V. Sernas, "Combined radiation and developing Laminar free convection between vertical flat plates with asymmetric heating," *J. Heat Transfer*, vol. 98, no. 1, pp. 95–100, 1976. ISSN 0022-1481. DOI: 10.1115/1.3450476.
[24] B. W. Webb and D. P. Hill, "High Rayleigh number Laminar natural convection in an asymmetrically heated vertical channel," *J. Heat Transfer*, vol. 111, no. 3, pp. 649–656, 1989. ISSN 0022-1481. DOI: 10.1115/1.3250732.
[25] O. Manca and V. Naso, "Experimental analysis of natural convection and thermal radiation in vertical channels," *ASME HTD*, vol. 145, nos. 13–21, p. 132, 1990.
[26] A. S. Krishnan, B. Premachandran, C. Balaji, and S. P. Venkateshan, "Combined experimental and numerical approaches to multi-mode heat transfer between vertical parallel plates," *Exp. Therm. Fluid Sci.*, vol. 29, no. 1, pp. 75–86, 2004. ISSN 0894-1777.
[27] R. Li, M. Bousetta, E. Chénier, and G. Lauriat, "Effect of surface radiation on natural convective flows and onset of flow reversal in asymmetrically heated vertical channels," *Int. J. Therm. Sci.*, vol. 65, pp. 9–27, 2013.
[28] C. Daverat, H. Pabiou, C.Ménézo, H. Bouia, and S. Xin, "Experimental investigation of turbulent natural convection in a vertical water channel with symmetric heating: Flow and heat transfer," *Exp. Therm. Fluid Sci.*, vol. 44, pp. 182–193, 2013.